Twentyfold blue upconversion emission enhancement through thermal effects in Pr 3+ /Yb 3+ -codoped fluoroindate glasses excited at 1.064 m

A. S. Oliveira, E. A. Gouveia, M. T. de Araujo, A. S. Gouveia-Neto, Cid B. de Araújo, and Y. Messaddeq

Twentyfold blue upconversion emission enhancement through thermal effects in Pr^{3+}/Yb^{3+}-codoped fluoroindate glasses excited at 1.064 μm

A. S. Oliveira, E. A. Gouveia, M. T. de Araujo, and A. S. Gouveia-Neto[a)]
Departamento de Física, Universidade Federal de Alagoas, Maceió 57072/970 AL, Brazil

Cid B. de Araújo
Departamento de Física, Universidade Federal de Pernambuco, Recife 50670/901, PE, Brazil

Y. Messaddeq
UNESP, Araraquara 14800/900, SP, Brazil

Infrared-to-visible upconversion emission enhancement through thermal effects in Yb^{3+}-sensitized Pr^{3+}-doped fluoroindate glasses excited at 1.064 μm is investigated. A twentyfold increase in the 485 nm blue emission intensity as the sample temperature was varied from 20 to 260 °C was observed. The visible upconversion fluorescence enhancement is ascribed to the temperature dependent multiphonon-assisted anti-Stokes excitation of the ytterbium sensitizer and excited-state absorption of the praseodymium acceptor. A model based upon conventional rate equations considering a temperature dependent effective absorption cross section for the $^2F_{7/2} \rightarrow ^2F_{5/2}$ transition of the Yb^{3+} and $^1G_4 \rightarrow ^3P_0$ excited-state absorption of the Pr^{3+}, agrees very well with the experimental results. © *2000 American Institute of Physics.* [S0021-8979(00)08209-8]

I. INTRODUCTION

Much interest has recently been devoted to the search for all-solid-state blue light sources for applications in high-density optical data reading and storage, undersea communications, and optical displays. An auspicious approach exploits infrared-to-visible frequency upconversion in Pr^{3+}-doped materials pumped by commercially obtainable infrared sources. Blue laser operation using frequency upconversion in the praseodymium-doped system has already been demonstrated in the single- and double-pumped configuration.[1–4] However, for the majority of rare-earth single-doped media the infrared-to-visible upconversion process has been proven inefficient, particularly for excitation in the 1.0–1.1 μm wavelength region, where high power laser sources are readily available. The realization of Yb^{3+}-sensitized materials, exploiting the efficient energy-transfer mechanism between the sensitizer and pairs or triads of rare-earth ions, has allowed a substantial improvement on the upconversion efficiency process in Tm^{3+},[5] Er^{3+},[6] and Pr^{3+} [5,7–10] doped systems. Nevertheless, new approaches to increase the upconversion efficiency are still under search.

In ytterbium-sensitized rare-earth doped materials, under infrared nonresonant excitation, with the pump-photon energy lower than the $^2F_{7/2} \rightarrow ^2F_{5/2}$ transition of the Yb^{3+} ion, the population of the acceptor visible emitting levels is accomplished via an indirect pumping process with multiphonon-assisted anti-Stokes excitation of the sensitizer,[11] followed by energy transfer to the acceptor in the ground state and a subsequent energy-transfer process to or absorption from the excited state. The excited-state absorption can be either resonant or multiphonon-assisted as in the case herein reported. Therefore, the effective pumping of the acceptor's emitting levels is strongly dependent upon the phonon population in the host material. In this work, we demonstrate both experimentally and theoretically that by heating nonresonant infrared excited fluoroindate glasses codoped with praseodymium and ytterbium in the temperature region of 20–260 °C, one obtains up to 20 times visible upconversion emission enhancement.

II. EXPERIMENTAL

The experimental investigation was carried out using fluoroindate glass samples with mol % composition of $(33.5-x)InF_3 – 20ZnF_2 – 20SrF_2 – 16BaF_2 – 6GaF_3 – 2NaF – 0.5PrF_3{}_{-x}YbF_3$. Fluoroindate glasses[12] have recently been the subject of much interest owing to their potential application in photonic devices based on rare-earth doped materials.[10,13] The material presents very good optical quality, is stable against atmospheric moisture, exhibits low optical attenuation from 250 nm to 8 μm, and due to the low maximum phonon-energy of $\sim$510 cm^{-1},[14] is expected to present significantly lower nonradiative decay rates as compared to fluorozirconate glasses ($\sim$590 cm^{-1}). The inclusion of GdF_3 and NaF in the glass composition has considerably reduced the devitrification process and improved the thermal stability, permitting the realization of fluoroindate glass fiber.[15] The samples had concentration of 5000 ppm/wt of praseodymium and different concentrations of ytterbium ions [5000(I), 10000(II), 15000(III) and 20 000(IV) ppm/wt]. The excitation source was a cw Nd:YAG laser operated at 1.064 μm. The pump beam was focused down into the samples by a 5 cm focal length lens and the pump beam waist at the samples location was $\sim$60 μm. The detection system consisted of a scanning spectrograph with operating resolution

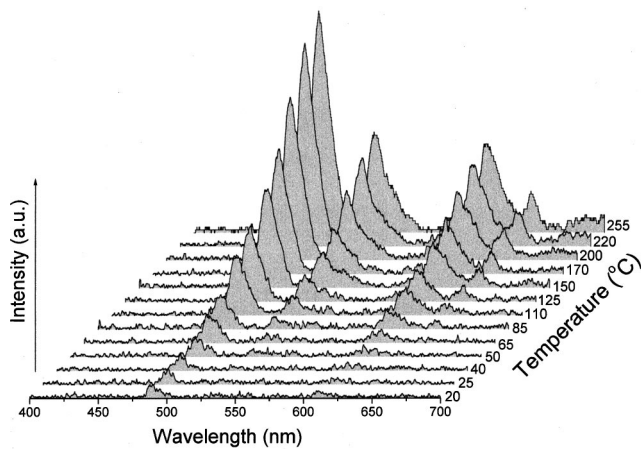a)Author to whom correspondence should be addressed; electronic mail: artur@fis.ufal.br

FIG. 1. Temperature evolution of the frequency upconversion emission spectrum. Excitation power of 400 mW at 1.064 μm. Sample IV.
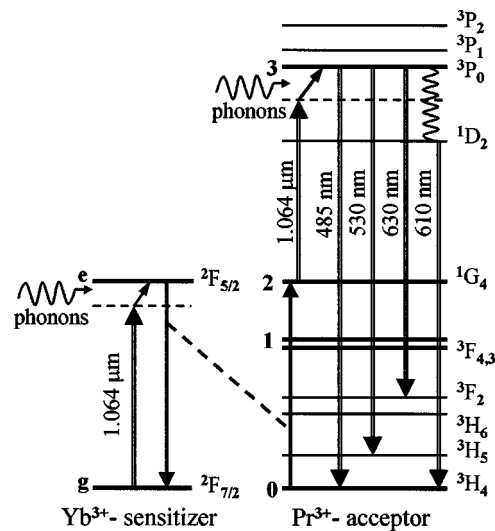

FIG. 2. Energy-levels scheme indicating participation of phonons in the absorption transitions. The solid lines connected by a dashed line represent the cross-relaxation process.

of 0.5 nm equipped with a S-20 uncooled photomultiplier tube coupled to a lock-in amplifier and computer. The temperature of the sample was increased from 20 to 260 °C by placing it into an aluminum oven heated by resistive wire elements. A copper-constantan thermocouple (reference at 0 °C) attached to one of the sample's faces was used to monitor the temperature within ~2 °C accuracy.

III. RESULTS AND DISCUSSION

Figure 1 illustrates the temperature evolution of the visible upconversion emission of light emanating from sample (IV) at a fixed excitation power of 400 mW at 1.064 μm. It can clearly be seen that the upconversion emission signals increased significantly as the sample's temperature was raised from 20 to 260 °C. The spectra depicted in Fig. 1 presented distinct emission bands centered around 485, 530, 610, and 630 nm corresponding to the $^3P_0 \rightarrow {}^3H_4$, $^3P_0 \rightarrow {}^3H_5$, $^1D_2 \rightarrow {}^3H_4$, and $^3P_0 \rightarrow {}^3F_2$ transitions of Pr^{3+} ions, respectively, with the blue signal obviously being the strongest. The $^3P_0 \rightarrow {}^3H_6$ transition can also contribute to the 610 nm fluorescence. Pumping of the Pr^{3+} excited-state visible emitting levels is accomplished through a combination of phonon-assisted absorption, energy transfer, and phonon-assisted excited-state absorption processes, as portrayed in the energy-level diagram depicted in Fig. 2. In the first step, a pump photon at 1.064 μm provokes a multiphonon-assisted anti-Stokes excitation of the Yb^{3+} sensitizer from the $^2F_{7/2}$ ground-state to the $^2F_{5/2}$ excited-state level. The excited Yb^{3+} transfers its energy to a neighbor Pr^{3+} ion in the $^3H_4$ ground state, exciting it to the $^1G_4$ level. This excited Pr^{3+} ion undergoes a multiphonon-assisted anti-Stokes excited-state absorption of a second pump photon, which promotes it to the $^3P_0$ upper emitting level. Finally, the excited Pr^{3+} ion decays from $^3P_0$ either radiatively to generate the main visible fluorescence emission bands or nonradiatively to populate lower-lying luminescent levels, as indicated in Fig. 2. The dependence of the blue emission intensity upon the excitation intensity at room temperature and at 115 °C was investigated and the results are presented in the log–log plot of Fig. 3. It was observed that the blue emission exhibited an

approximately quadratic power law behavior (slope ~2) with pump intensity. Within the excitation power range (up to 1.5 W) of our measurements, the results presented no indication of avalanche processes taking place. The avalanche process is characterized by a nonlinear dependence of the upconversion fluorescence emission upon the pump intensity with the existence of a critical pumping threshold.[8,16,17] However, we have observed a slope decrease in the emission intensity for pump powers above 700 mW at 115 °C, and 1.0 W at room temperature (20 °C). This behavior is in agreement with the power dependence of the $^3P_0$ population as will be demonstrated later on in this work.

The dependence of the blue emission at 485 nm upon temperature was examined for a fixed excitation power of 400 mW, and the results are presented in Fig. 4. As one observes, the 485 nm signal intensity increased by a factor of 20 in the temperature range of 20–260 °C. The 20× enhancement factor in the upconversion emission intensity was
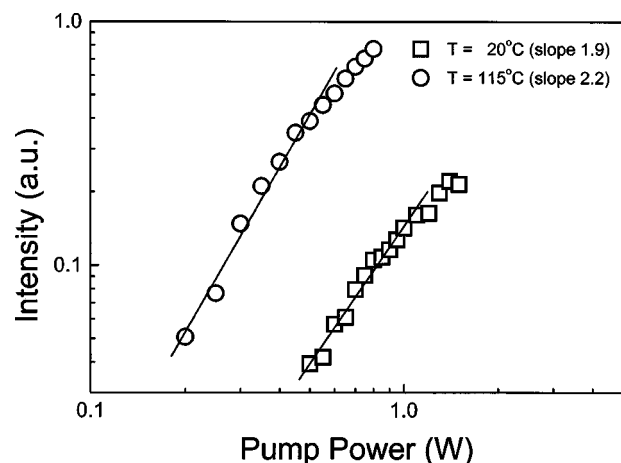

FIG. 3. Log–log plot of blue emission intensity as a function of the excitation power at room temperature (open squares) and at 115 °C (open circles), for sample IV.
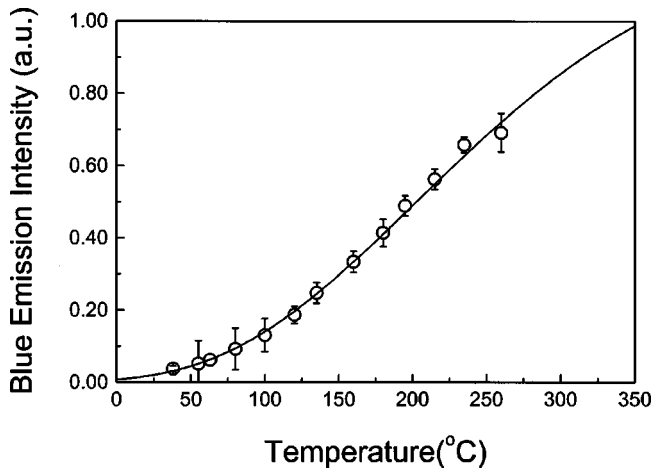
FIG. 4. Temperature dependence of the emission signal at 485 nm. Excitation power of 400 mW at 1.064 μm. Sample IV.

obtained by comparing the integrated spectrum around 485 nm at 260 °C and the one at room temperature (20 °C). As a matter of fact, we have not been able to quantify the infrared-to-blue conversion efficiency owing to the very small low power associated with the total visible fluorescence. Besides, we would have to both filter out the blue emission from the rest and collect that fluorescence in all directions. However, the enhancement is quite noticeable from the temperature evolution depicted in Fig. 1. This behavior can be explained as follows. The excitation of the Yb sensitizer from the $^2F_{7/2}$ ground state to the $^2F_{5/2}$ excited state requires the participation of at least two optical phonons in order to compensate for the energy mismatch of $\sim$800 cm^{-1} between the incident photon and the ytterbium transition energy. Furthermore, the praseodymium $^1G_4 \rightarrow {}^3P_0$ excited-state absorption also demands at least three phonons in order to match the energy difference of approximately 1450 cm^{-1} between the pump-photon energy and that of the Pr^{3+} transition. As a consequence, the population of the Pr^{3+} excited-state $^3P_0$ level relies strongly on the phonon occupation number in the host matrix. The multiphonon-assisted absorption leads to an effective absorption cross section for both sensitizer and acceptor, which are increasing functions of the sample temperature giving rise to the enhancement of the emitting levels populations.

The results are analyzed using a model that includes a phonon-assisted transition in the Yb^{3+} ion ($^2F_{7/2} \rightarrow {}^2F_{5/2}$), energy transfer to Pr^{3+} ($^2F_{5/2} \rightarrow {}^1G_4$), and subsequent phonon-assisted excited-state absorption to populate the $^3P_0$ level as portrayed in Fig. 2. Accordingly, the temperature dependence of the 485 nm emission intensity is described by the following set of rate equations:

$$\dot{n}_e = n_g \sigma_{ge}(T)\Phi - n_e C_{S2} n_0 - \frac{n_e}{\tau_S}, \quad (1a)$$

$$\dot{n}_2 = n_e C_{S2} n_0 - n_2 \sigma_{23}(T)\Phi - \frac{n_2}{\tau_2}, \quad (1b)$$

$$\dot{n}_3 = n_2 \sigma_{23}(T)\Phi - \frac{n_3}{\tau_3}, \quad (1c)$$

where $n_e C_{S2}$ is the sensitizer–acceptor energy-transfer rate, τ_S, τ_2, and τ_3 are the lifetimes of the levels $^2F_{5/2}$ (level e), $^1G_4$ (level 2), and $^3P_0$ (level 3), respectively, and Φ is the power flux. In Eqs. (1), $\sigma_{ge}(T)$ and $\sigma_{23}(T)$ represent the temperature dependent effective absorption cross sections for the Yb^{3+} excitation and Pr^{3+} excited-state absorption, respectively, owing to the so called multiphonon-assisted anti-Stokes excitation process.[11] The absorption cross sections can be written in a general form as

$$\sigma(T) = \sigma^0[\exp(h\nu_{phonon}/k_B T - 1)]^{-p}, \quad (2)$$

where σ^0 is the absorption cross section at resonance, $h\nu_{phonon}$ is the phonon energy, k_B is the Boltzmann constant, and T the absolute temperature. The exponent p accounts for the number of phonons taking part in the anti-Stokes absorption processes. Combining the above equations, one obtains the steady-state population of the blue emitting level as

$$n_3 \cong \frac{\tau_2 \tau_3 \tau_S \sigma_{23}(T) N_A N_S C_{S2} \sigma_{ge}(T)\Phi^2}{[1 + \tau_S \sigma_{ge}(T)\Phi + \tau_S N_A C_{S2}]}, \quad (3)$$

where N_A and N_S are the Pr^{3+} and Yb^{3+} concentrations, respectively. In order to derive Eq. (3), we have neglected the cross-relaxation mechanism ($^3P_0, {}^2F_{7/2}) \rightarrow ({}^1G_4, {}^2F_{5/2}$) from the pair Pr^{3+}–Yb^{3+}, for which one would expect that the lifetime of the $^3P_0$ level depends upon the Yb^{3+} concentration and such a behavior was not observed in Pr^{3+}/Yb^{3+}-doped fluoroindate glasses.[10] We could also exclude cooperative upconversion of Yb ions since we have observed that the visible fluorescence intensity presented a linear dependence with the concentration of Yb^{3+}. We have assumed that back transfer from $^1G_4$ to $^2F_{5/2}$ does not play a significant role as in the case of ZBLAN.[18] Finally, we estimated $\sigma_{23}\Phi \ll \tau_2^{-1}$ (fulfilled by our experimental conditions) using data from Ref. 19, which implies that a small fraction of Pr^{3+} is excited, leading to $n_0 \approx N_A$. The blue light intensity at 485 nm is then given by $I_{485nm} = h\nu_{30} A_{30} n_3$, where A_{30} is the radiative transition rate from level 3 to the ground state and ν_{30} its frequency.

To obtain the temperature dependence of the blue emission intensity through Eq. (3) further considerations need to be made. The lifetime of the $^2F_{5/2}$ level is mainly radiative due to the large energy separation from ground state (10256 cm^{-1}). The nonradiative transitions from $^1G_4$ (9696 cm^{-1}) to lower-lying levels are expected to be small, as compared to the excited-state pumping rate $^1G_4 \rightarrow {}^3P_0$ and due to the low maximum-phonon energy associated with fluoroindate hosts,[14] which requires the participation of at least six optical phonons to bridge the energy gap (3245 cm^{-1}) connecting the levels $^1G_4 - {}^3F_{3,4}$, resulting in negligible nonradiative transition probability.[17] This means that the lifetimes τ_s and τ_2 are approximately temperature independent. Moreover, the energy-transfer rate $N_S C_{S2}$ is very high for samples III and IV (Ref. 10) and it is also temperature dependent because of the energy mismatch ($\Delta E_{e2} = 560$ cm^{-1}) between the $^2F_{5/2}$ level of Yb^{3+} and the $^1G_4$ level of Pr^{3+}, and this dependence can be accounted through $\exp(-\Delta E_{e2}/k_B T)$ according to Ref. 11. Finally, the lifetime of the $^3P_0$ is related to nonradiative transition probabilities $W_{NR}(T)$ through
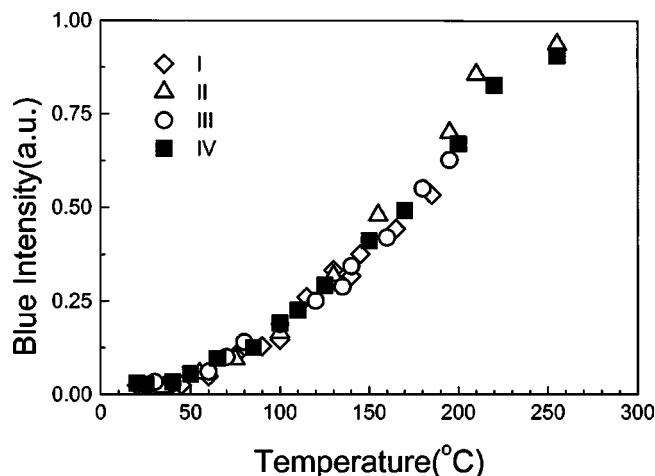
FIG. 5. Temperature dependence of the blue emission efficiency for samples I–IV, at a fixed pump power, normalized to the Yb^{3+} concentration.

$$\tau_3^{-1} = \sum_j A_{3j} + W_{NR}(T), \qquad (4)$$

and for low concentrations of rare-earth ions, $W_{NR}(T)$ is due to multiphonon relaxation processes, and can be related to the temperature through[11,20]

$$W_{NR}(T) = W_{NR}(0)[1 - \exp(-h\nu_{shonon}/k_B T)]^{-p}, \qquad (5)$$

where $W_{NR}(0)$ is its value at zero temperature and the exponent p is the phonon order linking the $^3P_0$ level (20367 cm^{-1}) to the next lower energy level $^1D_2$ (16942 cm^{-1}). Using the experimental lifetime $\tau_3(28\,\mu s)$ for the $^3P_0$ at room temperature[10] and radiative transitions rate from Ref. 21 for our samples, one is left with a value of $W_{NR}(300\,K) = 24\,767\,s^{-1}$, which means that the $^3P_0$ level can populate the $^1D_2$ level very efficiently.

We have obtained the temperature dependence of the blue emission intensity by adjusting the phonon energy, and the result is illustrated by the solid line in the plot of Fig. 4. As can be observed, indeed the theoretical model matches the experimental results very well. By using a similar approach, we have recently described a fourfold upconversion emission enhancement in Er^{3+}/Yb^{3+}-codoped chalcogenide glasses and the theoretical model based upon multiphonon-assisted anti-Stokes excitation of the nonresonant pumping of the sensitizer has also proven to agree very well indeed with the experimental data.[22] The theoretical fitting of data depicted in Fig. 4, also permitted us to withdraw the value of ~ 400 cm^{-1} for the phonon mode participating in the multiphonon-assisted anti-Stokes excitation and excited-state absorption of the sensitizer and the acceptor, respectively. However, it can be inferred that there exists a deviation of ~ 110 cm^{-1} from the value for the maximum phonon energy associated with fluoroindate glasses.[14] The deviation is attributed to the fact that in anti-Stokes sideband excitation processes,[11] one has to consider an effective phonon mode, which possesses lower energy than the cut-off one. The phonon population distribution directly involved in the anti-Stokes excitation mechanism is centered around the so called ''effective-phonon-mode,'' as has recently been realized.[23]

We have also performed the same set of experiments using samples I–III, and the results exhibited basically the same behavior as far as blue emission intensity temperature dependence is concerned, as can be inferred from the experimental data depicted in Fig. 5. The upconversion emission efficiencies have followed the same trend with an overall maximum enhancement of approximately $\times 20$ for all samples. However, the lower ytterbium concentration samples required higher pump powers, in order to obtain appreciable upconversion fluorescence visible signals, as a result from the linear intensity dependence with Yb^{3+} concentration.

CONCLUSION

In conclusion, the experimental and theoretical investigation of thermally induced infrared-to-visible upconversion fluorescence emission enhancement in Yb^{3+}/Pr^{3+}-doped fluoroindate glasses excited at 1.064 μm was examined for the first time. Our results revealed a 20-fold enhancement in the 485 nm blue emission intensity as the temperature of the glass sample was varied in the 20–260 °C range. The upconversion emission enhancement was assigned to a temperature dependent effective absorption cross section for the sensitizer excitation and acceptor excited-state absorption. The model based upon conventional rate equations considering the absorption cross sections of both sensitizer and acceptor as functions of the phonon population in the host matrix, has proven to agree very well with experimental data. The results indicated that the heating process can be exploited to improve power performance (times four output power increase and threshold reduction) of Er/Yb-doped fiber lasers pumped by high power sources in the 1.0 μm spectral region, and also enhance gain by 60% in a single-pass visible light amplification mechanism in Er/Yb-codoped chalcogenide glass pumped at 1.064 μm, as has recently been demonstrated in our lab.[24,25]

ACKNOWLEDGMENTS

[1] J. Y. Allain, M. Monerie, and H. Poignant, Electron. Lett. **26**, 166 (1990).
[2] R. G. Smart, D. C. Hanna, A. C. Tropper, S. T. Davey, S. F. Carter, and D. Szebesta, Electron. Lett. **27**, 1307 (1994).
[3] Y. Zhao and S. Poole, Electron. Lett. **30**, 967 (1994).
[4] Y. Zhao, S. Fleming, and S. Poole, Opt. Commun. **114**, 285 (1995).
[5] D. C. Hanna, R. M. Percival, I. R. Perry, R. G. Smart, J. E. Townsend, and A. C. Tropper, Opt. Commun. **78**, 187 (1990).
[6] Y.-M. Hua, Q. Li, Y.-L. Chen, and Y.-X. Chen, Opt. Commun. **88**, 441 (1992).
[7] D. M. Baney, G. Rankin, and K. W. Chang, Appl. Phys. Lett. **69**, 1662 (1996).
[8] T. R. Gosnell, Electron. Lett. **33**, 411 (1997).
[9] D. M. Baney, G. Rankin, and K. W. Chang, Opt. Lett. **21**, 1372 (1996).
[10] W. Lozano B., C. B. de Araújo, C. E. Egalon, A. S. L. Gomes, B. J. Costa, and Y. Messaddeq, Opt. Commun. **153**, 271 (1998); L. E. E. de Araújo, MSc. thesis, Universidade Federal de Pernambuco, Brazil, 1994.

4278   J. Appl. Phys., Vol. 87, No. 9, 1 May 2000

Oliveira *et al.*

[11] F. Auzel, Phys. Rev. B **13**, 2809 (1976).

[12] Y. Messaddeq and M. Poulain, Mater. Sci. Forum **67–68**, 161 (1989).

[13] See, for example W. Lozano B, C. B. de Araújo, L. H. Acioli, and Y. Messaddeq, J. Appl. Phys. **84**, 2263 (1998); E. Martins, C. B. de Araújo, J. R. Delben, A. S. L. Gomes, B. J. da Costa, and Y. Messaddeq, Opt. Commun. **158**, 61 (1998); G. S. Maciel, L. de S. Menezes, C. B. de Araújo, and Y. Messaddeq, J. Appl. Phys. **85**, 6782 (1999), and references therein.

[14] R. M. Almeida, J. C. Pereira, Y. Messaddeq, and M. Aegerter, J. Non-Cryst. Solids **161**, 105 (1993).

[15] Fibers of fluoroindate glass have been developed by Le Vèrre Floré (France) since 1998—M. Poulain (private communications).

[16] T. Sandrock, H. Scheife, E. Heumann, and G. Huber, Opt. Lett. **22**, 808 (1997).

[17] J. S. Chivian, W. E. Case, and D. D. Eden, Appl. Phys. Lett. **35**, 124 (1974).

[18] P. Xie and T. R. Gosnell, Electron. Lett. **31**, 191 (1995).

[19] R. S. Quimby and B. Zheng, Appl. Phys. Lett. **60**, 1055 (1992).

[20] M. J. Weber, Phys. Rev. B **8**, 54 (1973).

[21] A. Flórez, O. L. Malta, Y. Messaddeq, and M. A. Aegerter, J. Non-Cryst. Solids **213&214**, 315 (1997).

[22] P. V. dos Santos, E. A. Gouveia, M. T. de Araujo, A. S. Gouveia-Neto, A. S. B. Sombra, and J. A. Medeiros Neto, Appl. Phys. Lett. **74**, 3607 (1999).

[23] F. Auzel and Y. H. Chen, J. Lumin. **66/67**, 224 (1996).

[24] C. J. da Silva, M. T. de Araujo, E. A. Gouveia, and A. S. Gouveia-Neto, Opt. Lett. **24**, 1287 (1999).

[25] S. F. Felix, E. A. Gouveia, M. T. de Araujo, A. S. B. Sombra, and A. S. Gouveia-Neto, J. Lumin. (to be published).